

THREE-DIMENSIONAL GEOMETRICAL OPTICS CODE FOR INDOOR PROPAGATION

Christopher W. Trueman

Electromagnetic Compatibility Laboratory, Concordia University,
7141 Sherbrooke Street West, Montreal, Quebec, Canada H4B 1R6

Abstract - This paper presents program GO_3D for computing the fields of a transmitter in an indoor environment using geometrical optics. The program uses an “image tree” data structure to construct the images needed to compute all the rays carrying fields above a preset “threshold” value, no matter how many reflections are needed. The paper briefly describes the input file required to define wall construction, the floor plan, the transmitter, and the receiver locations. A case study consisting of a long corridor with a small room on one side is used to demonstrate the features of the GO_3D program.

I. Introduction

Propagation of radio waves in an indoor environment has become important because of the widespread use of wireless technology. Cellular telephones are frequently used indoors and must communicate with base stations located on nearby buildings or towers. Security guards use walkie-talkies. Wireless LANs are used to network computers and printers without the need for expensive, messy wiring that is costly to reconfigure. For adequate communication, the signal strength at the receiver due to a transmitter elsewhere in the building must exceed a minimum value. Conversely, electromagnetic interference or EMI can result if the signal strength of a transmitter exceeds the maximum permissible field strength or “immunity” of another device. EMI is of particular concern in hospital environments where medical equipment may malfunction, with grave consequences, if the signal strength of a cellular phone or walkie-talkie is larger than the immunity level, typically 3 V/m [1].

Geometrical optics (GO) is often used to construct detailed, realistic maps of the signal strength in an indoor environment [2-7]. In GO, rays are traced from the transmitter location to the receiver location. Walls are modeled as planar, layered panels. Rays can reflect from walls and must obey Snell’s Law at the reflection point. Reflection points are often found by constructing the image of the source in the wall panel. The reflection process is treated as “local”, meaning that the incoming and reflected waves are considered to be plane waves, and so plane wave reflection coefficients are used. Plane wave reflection and transmission coefficients are available for homogeneous panels of a given material and thickness and for panels which are constructed of layers of material, each with given

electrical properties and thickness [8]. Coupling paths from the transmitter to the receiver may involve two, three or many reflections from the walls, and can be tracked using a tree data structure of image sources [3]. The field arriving at the receiver is the sum of the fields associated with all the rays that arrive there. In an indoor environment, waves usually arrive from many different directions, having followed ray paths with a wide range of path lengths. Still, GO can find a vector sum of all the fields, and so find the vector components E_x , E_y and E_z of the field at any given location. Geometrical optics has the disadvantage that the field strength contains discontinuities that arise when rays abruptly disappear. Adding edge diffractions [2,3] smoothes the fields, but complicates and slows down the ray tracing program. The accuracy of geometrical optics for indoor propagation has been assessed against measured field strengths in Ref. [7].

This paper presents a three-dimensional geometrical optics program for indoor propagation called “GO_3D”. The user defines the floor plan, using layered wall construction, by specifying the locations of the wall panels. The transmitter is specified either as a dipole antenna, or with a file of radiation patterns computed with an antenna-analysis program. The user defines points at which GO_3D must find the field, called “receivers”. GO_3D requires the user to specify a threshold value, used to compute a cutoff field strength, and all the rays with field strengths greater than the cutoff are included in the computation. GO_3D constructs the tree of image sources once and then uses the same tree to find the rays at all of the receivers. GO_3D uses a fully three-dimensional, vector calculation accounting for the magnitude and phase of both vector field components associated with each ray. For a single observer, the program creates graphics showing the ray paths, and a file giving the field strength and path length for each ray. For lines of receivers, the field strengths E_x , E_y , E_z and E_r can be graphed as a function of distance. For grids of receivers, each field component can be graphed as a contour map. The GO_3D program and a User’s Guide is available on-line [9].

II. The Ray Tracing Algorithm

This section briefly describes the ray tracing method used by the GO_3D computer code. Fig. 1 illustrates the construction of the set of images for a transmitter “Tx” and

a system of three walls, leading to the “image tree” data structure shown in Fig. 2. The 1st level of the tree contains the image of the transmitter in each of the

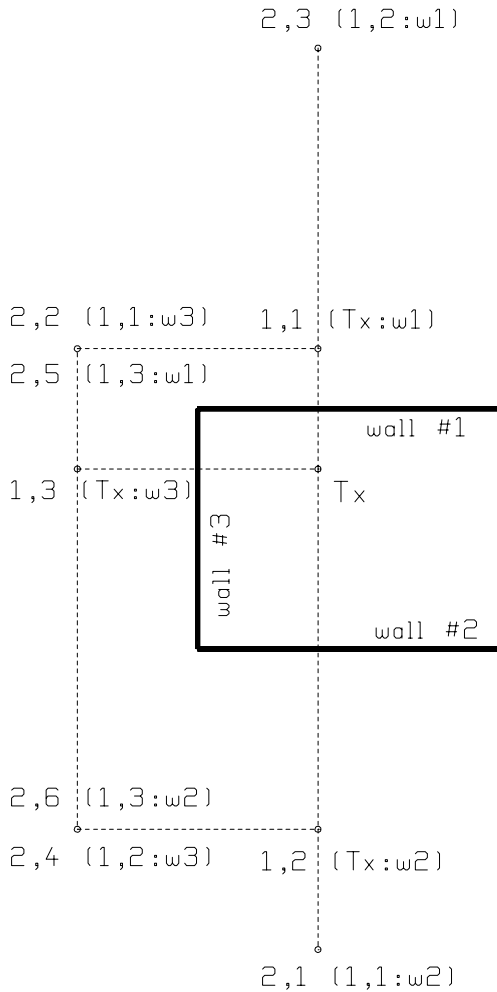


Fig. 1 A system of three walls and a transmitter (Tx). The first two levels of images are shown.

three walls, labelled as sources (1,1), (1,2) and (1,3). Also, the source generating the image has been identified as “Tx” in each case, and the wall identified as “w1” for wall #1, etc. Images at level i in the tree are numbered sequentially, $j=1,2,3$, so each image is identified by an ordered pair (i,j) . For our system of three walls, these three 1st level image sources are sufficient to compute all ray paths having one reflection from the transmitter to the observer. The 2nd level of the tree contains the image of each 1st level source in each wall, except the wall that created the 1st level image. Thus, image source (1,1) is an image in wall #1, and generates 2nd level image (2,1) in wall #2, and image (2,2) in wall #3. Similarly, imaging source (1,2) obtains images (2,3) and (2,4); and imaging (1,3) gets (2,5) and (2,6) for a total of 6 image sources at the second level, as shown in Fig. 1. This is sufficient to compute all ray paths

with one reflection or with two reflections from the transmitter to the observer. The third level has the image of six 2nd level sources in two walls, for a total of twelve images. Note that the image tree is correct for *any* location of the observer, so the *same* image tree can be used to find the field for all possible observers.

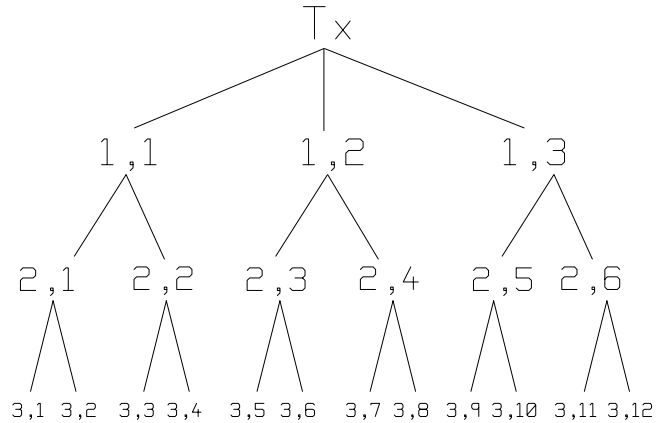


Fig. 2 The image tree showing the transmitter and three levels of images.

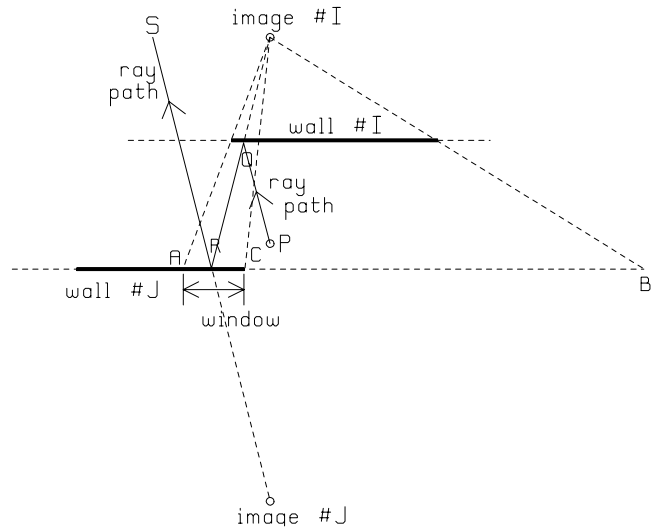


Fig. 3 An image source I and its image J in wall #J.

A. The Image’s Window

With M walls, there are M images at the 1st level, $(M - 1)M$ images at the 2nd level, $(M - 1)^2 M$ images at the 3rd level, and so forth, and the number of image sources at each level grows rapidly. However, some image sources can be discarded immediately because the walls are not *infinite* planes. Consider the configuration in Fig. 3, where

image source #I is an image in wall #I, and at the next level, image source #J is an image of source I in wall #J. The projection of wall #I from image source #I onto wall #J is segment AB in the plane of wall #J. In three dimensions this is an area. The portion of AB that lies within the physical area of wall #J is segment AC, and is called the “window” associated with image source #J in wall #J. A ray from image source #J must pass through the “window” to be physically possible. Thus the ray from some source at P, reflected at Q from wall #I, reflected at R from wall #J, and reaching an observer at S, is physically possible. If the segment AB on the plane of wall #J does not intersect any part of wall #J, then the window is of zero extent and image source #J can be discarded as the image tree is constructed. This eliminates a great many image sources from the tree.

In carrying out ray tracing from a source at P to an observer at S, first a ray is traced from observer S to image J. The intersection of this ray with the plane of the wall #J at point R must lie within image #J’s window, which is line segment AC, or else the ray can be discarded. If the ray is possible, then the ray is traced back to image source I, by joining reflection point R to source #I. The intersection of the ray from I to R with the plane of wall #I must lie within the “window” of image source #I(not shown on the figure), or else the ray can be discarded. If it does then reflection point Q is joined with source, P, and a two-reflection ray path has been found. Thus each entry in the image tree contains the 3D coordinates of an image source, and the size and location of the image’s window. The image source looks out on the world through the window, meaning that rays from the image source must pass through the window to be physically possible.

In constructing the image tree, it will be found that many image sources have a window of zero extent and so can be discarded from the tree. Thus the concept of “window” eliminates many images from the tree but is not sufficient as a stopping criterion. The GO_3D code uses a minimum field strength associated with an image source to terminate the image tree, as explained in the following.

B. The Threshold

Ideally a geometrical optics analysis should track each ray through many reflections and transmissions until it exits from the problem space. But at each reflection, there is a transmitted ray, which must also be traced through many reflections until it exits from the problem space. The computation quickly becomes very time-consuming and expensive. For most wall materials, the field strength associated with the ray is substantially reduced either when the ray penetrates a wall or when the ray reflects from a wall. After a number of reflections the field strength associated with a ray might be expected to be negligible, and the ray can be discarded, and not tracked any further. Many geometrical optics computer codes discard rays after a fixed number of reflections, say 3, 6 or 10. But for

example for near-grazing incidence, the reflection coefficient approaches unity for any type of wall construction and a ray can be reflected many times without much loss of field strength. This can happen, for example, in computing the field in a long corridor [10].

The GO_3D code uses a different criterion for discarding rays. Each ray is traced through as many reflections as required to reduce its estimated field strength to less than the “cutoff” field strength E_{cutoff} . If the transmitter radiates P_{rad} watts of power then the amplitude of the “isotropic level” field strength is

$$E_{iso} = \sqrt{\frac{\eta_0 P_{rad}}{2\pi}} \approx \sqrt{60P_{rad}}$$

The user specifies to the GO_3D code a threshold T in dB below the isotropic level. The cutoff field strength is then

$$E_{cutoff} = E_{iso} 10^{-(T/20)}$$

For a 600 mW source, the isotropic level is 5.998 V/m, or about 6 V/m. A threshold of $T = 20$ dB with a 600 mW source instructs the code to discard image sources having fields less than $E_{cutoff} = 0.6$ V/m. An image source is included in the calculation if the largest field strength it can give rise to, for any observer, is greater than or equal to the “cutoff” field strength. The code will construct the image tree to as many levels as needed to include all such sources.

In practice, the GO_3D code constructs the image tree once, after the input geometry file has been read, and then uses the same image tree for all the receiver positions. Thus, the location of an observer cannot be a criterion for whether an image should or should not be included in the image tree. The field an image source gives rise to is of the form

$$E = E_0 \frac{A}{r}$$

where E_0 is the strength of the transmitter in the direction associated with the image source, A is the net attenuation along the path including the reflection loss when the ray is reflected from walls and the transmission loss when the ray penetrates walls. Distance r is the *minimum* possible distance from the source to the observer; hence the observer location that is closest to the image source is used. To decide whether to include or discard an image, the GO_3D code uses $E_0 = E_{iso}$, the source’s isotropic level, and assumes no loss of amplitude due to transmission or reflection, $A = 1$, which is the worst case. An image is retained if

$$\frac{E_{iso}}{r} \geq E_{cutoff}$$

or equivalently if $r \leq r_{cutoff}$ where the cutoff distance is $r_{cutoff} = E_{iso}/E_{cutoff}$. Thus, the decision of whether to retain or discard an image in the image tree is based simply on the nearest possible distance from the image source to an observer.

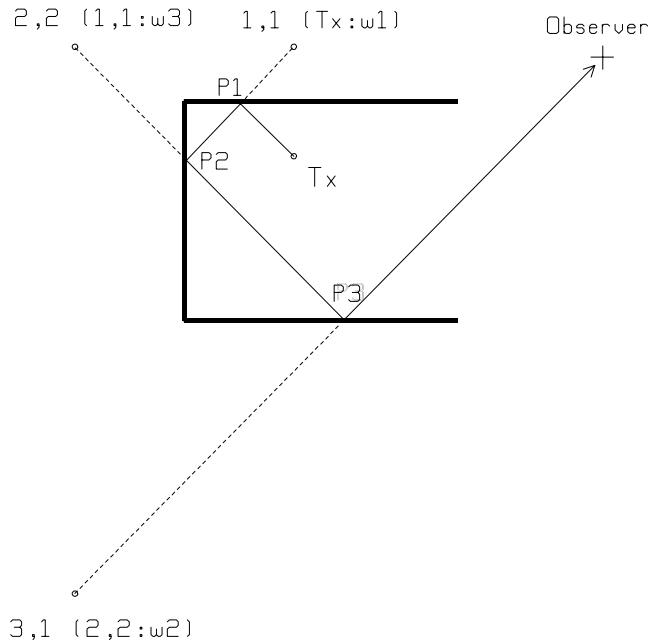


Fig. 4 Tracing a ray using the image tree.

C. Tracing Rays to an Observer

In a typical calculation, the field is required at many points along a line, or at many points covering a rectangular grid. Each such point is a “receiver”. Consider the image tree of Fig. 2, with three levels. To trace all possible rays the program must start with each individual image source, and try to trace a ray from the receiver, via that source, back through the image tree to the transmitter. The ray-tracing procedure for image (3,3) is shown in Fig. 4. Join the receiver R_x to image (3,3) with a ray and find intersection P_3 . If P_3 does not lie within the “window” of image (3,3) discard the ray path and move on to the next image source. But if P_3 lies within the window then join P_3 to the “parent” image in the tree of Fig. 2, namely image (2,2). If reflection point P_2 lies within the window of image (2,2), then join P_2 to the “parent” in the tree, which is image (1,1), to find P_1 . If P_1 lies in the window of image (1,1), then join P_1 to the parent, which is the transmitter. Then path T_x to P_1 to P_2 to P_3 to R_x is a ray path. To find the field at the observer, find the vector components of the transmitter’s field along path T_x to P_1 , accounting for the directional antenna patterns and polarization of the transmitter. The dyadic reflection coefficient at P_1 accounts for the reflection coefficient for the “parallel” and “perpendicular” components of the field at the reflection point, and for the angle of incidence from the normal. Similarly, the dyadic reflection coefficients are used at P_2 and P_3 , and finally the ray is “propagated” to the observer. The result is the magnitude and phase of the

three vector components of the field, E_x , E_y and E_z , at the receiver on a three-reflection path using image source (3,3). The process must be repeated for all the image sources at level 3; this finds all possible three-reflection paths. Then look for two-reflection paths starting with image source (2,1), considering all 2nd level image sources in turn. This finds all possible two-reflection paths. Then consider each 1st level image in turn to find one reflection paths. Finally the direct path from the source is found. Adding the fields due to all the rays that are found obtains the net field strength at the observer. In general, some rays will penetrate walls in the floor plan. When a ray penetrates a wall, its field strength is reduced by applying the dyadic transmission coefficient to the ray’s two field components.

The search for ray paths using the image tree is repeated for each “receiver” that the user has specified.

III. The GO_3D Input File

The user of the GO_3D program must prepare a text file, with extension “go3”, which describes the construction and location of the walls, gives the frequency and location of the transmitter, and defines the position of “receivers” where the field must be calculated. The program uses a descriptive input “language” and encourages users to annotate their “go3” files liberally with comments for later reference. A detailed description of the input language including a comprehensive example can be found in Ref. [9]. The following provides an introduction.

Materials out of which walls are to be built are defined by name, such as “Concrete”, and the permittivity, conductivity and permeability of each material are given, at the operating frequency. Layered wall construction is defined by name, such as “SheetrockWall”, by giving the thickness of each layer and invoking the material of the layer by name, such as “Concrete” or “Space”. The floor plan is then defined by specifying the location of wall panels and invoking the wall construction of each panel by name. In GO_3D, wall panels must be parallel to the coordinate planes. Usually, the floor plan is built up a few walls at a time, and the GO_3D code is run with no receivers defined to obtain the plan and elevation view shown in Fig. 5. The location of the newly-added wall panels can be checked, then a few more added, and their locations checked again. In this way errors in the input file are corrected as they are made. A floor is added under all the walls by naming the material of the floor (such as “Concrete”) and giving the thickness. This permits ray paths that reflect from the floor as well as from various wall panels in traveling from the transmitter to the receiver. A flat ceiling can be added as well. However, many real buildings have a hanging ceiling which conceals a complex array of conduits, air ducts, wiring, and pipes for plumbing. Such a ceiling does not reflect spectrally, but rather scatters

the field in a complex way. A uniform, smooth ceiling is a poor model.

The user must specify the operating frequency in MHz, the power radiated by the transmitter in mW, and the location of the transmitter. There are two options for modeling the source itself. The source can be a half-wave dipole oriented in a user-specified direction. Or the source antenna can be described with an input file containing values of the field components E_θ and E_ϕ over the surface of the radiation sphere. Such a file is readily created with an antenna analysis program based in finite element analysis, or the moment method, or the finite-difference time-domain method. The User's Guide [9] gives the details of the format required for this input file. Thus, a cellular telephone handset operating near the head can be solved with FDTD, and the radiation patterns imported into GO_3D for an indoor propagation study.

To find the field strengths with GO_3D, the user must specify the threshold in dB below the isotropic level. This is a "control" that determines the number of levels in the image tree and so the number of ray paths that the program looks for. The change in the field strength as the threshold is increased is discussed below for the hallway and room problem of Fig. 5.

The locations at which the field is to be computed are called "receivers". Receivers can be defined along a line joining any two points in space, or can be evenly spaced over a grid parallel to one of the coordinate planes. The program creates an output file containing a table giving the location of each receiver, and the magnitudes of E_x , E_y , E_z , and the "total field" E_t , defined by

$$E_t = \sqrt{(|E_x|^2 + |E_y|^2 + |E_z|^2)}$$

The total field formula ignores the phase information. It represents the worst-case field strength that would arise if all the field components were in phase, and is used to assess the worst-case EMI risk. GO_3D can create files in the "native format" for "RPLOTT" for graphing field strength along a line, or for "CPLOTT" for drawing color contour maps of field strength over a grid. These programs are available as part of the User's Guide [9]. Or GO_3D can create "generic" output files for the user's favorite graphing software.

IV. The Corridor and Room Problem

The hallway with a small side room of Fig. 5 will be used to demonstrate the features of the GO_3D program. Figure 5 shows a floor plan or xy plane view in the lower part of the figure and an elevation or xz plane view in the upper part. The floor plan consists of a corridor 20 m long and about 2 m wide. One room off the corridor is included in this simple floor plan. The doorway is 1 m wide, with a wood door, 10 cm thick, in the "open" position. The room measures about 3 by 4 m. The room has a window which

is modeled with a glass "wall panel" of appropriate thickness and electrical properties. The lower half of the window is covered with a metal screen, which was included in the model as a thin metal "wall panel" of appropriate size and location. There is a transmitter in the corridor that represents an 850 MHz cell phone radiating 600 mW. The cell phone's radiation patterns will be modeled with those of a vertical, half-wave dipole, at a height of 1.6 m above the floor. The problem is to determine the field strength in the room, for instance along the path indicated by the dashed line in Fig. 5, starting near the center of the doorway and ending near the window.

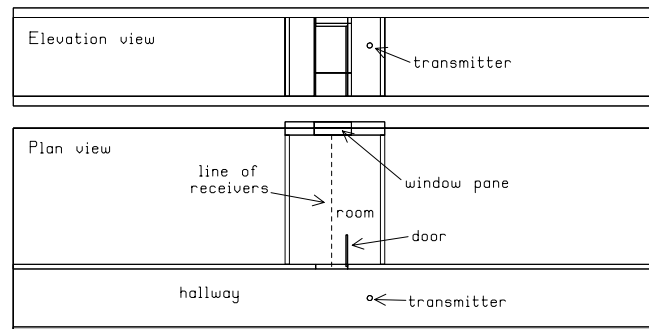


Fig. 5 A hallway with a side room.

A. Reflection Coefficient

Knowledge of the behaviour of the reflection coefficient of each type of wall construction can be useful in understanding the fields that result when rays are incident upon the wall. The GO_3D program creates files giving the dependence of the reflection coefficient on both the frequency and the angle of incidence of the plane wave on the wall.

Four types of wall construction are studied in Figs. 6 and 7. A "brick wall" is a solid, 14 cm layer of brick material having $\epsilon_r = 5.1$, $\sigma = 10$ mS/m at 850 MHz. A "sheetrock wall" consists of surface sheets of drywall 1 cm thick, separated by a 12 cm air layer. The drywall is represented with the electrical properties of concrete, $\epsilon_r = 6.1$, $\sigma = 60.1$ mS/m. A "clay block wall" models a real wall construction using hollow clay blocks faced with plaster. This is represented as a layered structure with a 1.5 cm plaster (concrete) facing, a 0.8 cm layer of brick representing the wall of the clay block, a 9.4 cm thick air space inside the clay block, the 0.8 cm block wall and the 1.5-cm plaster facing on the other side of the wall. Some clay block walls have metal screen embedded within the plaster. A "plaster and wire wall" models a 1 cm thick plaster (concrete) facing backed by a very highly conducting metal layer.

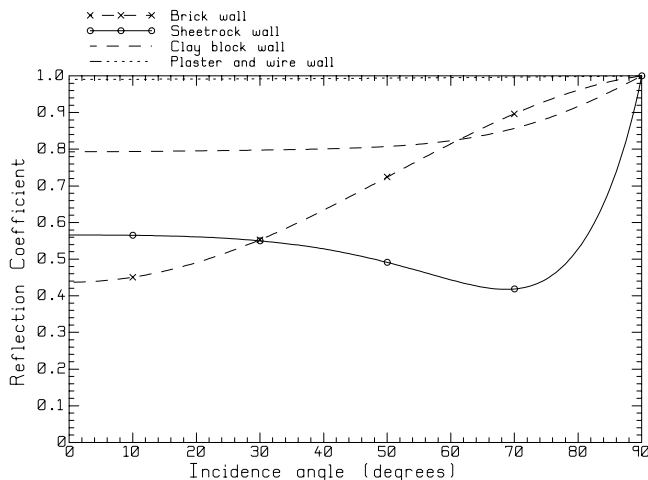


Fig. 6 The reflection coefficient as a function of the incidence angle.

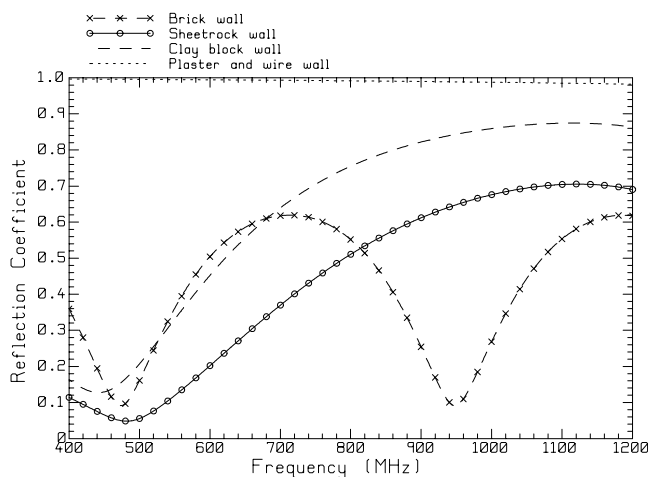


Fig. 7 The reflection coefficient as a function of frequency.

Figure 6 shows the reflection coefficient for the perpendicular polarization as a function of the angle of incidence from the normal, for the four types of wall construction, at the operating frequency of 850 MHz. Grazing incidence corresponds to 90 degrees from the normal, and all the wall constructions have a reflection coefficient of unity at grazing. Hence, in a long corridor with the transmitter at one end and the receiver at the other, rays following zig-zag paths will be incident at near grazing and so will be reflected with little attenuation at each reflection. Fig. 6 shows that the “plaster and wire” wall is almost perfectly reflecting. The brick and the clay block constructions have reflection coefficients which rise with increasing incidence angle. Although the brick wall is the heavier construction, its reflection coefficient is only 0.44 for normal incidence compared to 0.79 for the lighter clay block construction. The lightest construction is the sheetrock wall, yet its reflection coefficient at normal incidence is 0.57, larger than the much-heavier brick wall.

Also, note that the sheetrock wall’s reflection coefficient declines with incidence angle, to a minimum of about 0.42 at an incidence angle of 70 degrees from the normal. For angles nearer grazing the reflection coefficient rapidly rises to unity. Single-layer walls can be almost transparent for incidence in the parallel polarization at the “Brewster angle”, where the wall behaves as a “Brewster window”, with zero reflection coefficient.

The frequency dependence of the reflection coefficient explains why for heavy wall constructions it can be less than that for a light construction, as follows. Fig. 7 shows the reflection coefficient for normal incidence for the four wall types, as a function of frequency. The wall construction with an embedded wire mesh has a near-unity reflection coefficient across the frequency band. The reflection coefficient for all of the layered wall constructions varies strongly with frequency, with minima where the value of the reflection coefficient is quite small. For normal incidence on solid walls made of low loss materials such as brick, the wall is almost transparent at frequencies where its thickness is an integer multiple of the half-wavelength. The wall behaves as a radome and the field passes through it with little attenuation. Fig. 7 shows that the 14 cm brick wall has “radome frequencies” at 475 and 950 MHz. The maximum reflection coefficient for normal incidence is at about 710 MHz and is 0.62. It violates our intuition that from 710 to 950 MHz the wall is getting thicker in terms of the wavelength but the reflection coefficient is decreasing. It is also against our intuition that a “light” wall construction such as sheetrock can have a higher reflection coefficient at 0.57 at 850 MHz than a “heavy” wall construction such as solid brick, with 0.44. Fig. 7 shows that multiple-layer walls can also have “radome” frequencies; thus the clay block wall has a minimum reflection coefficient at 444 MHz. The frequency interval between minima tends to be larger for layered constructions.

To characterize the reflective properties of each wall construction in a single number, the reflection coefficient for the “perpendicular” polarization can be averaged over all angles of incidence. The lightest wall construction is sheetrock, with an average reflection coefficient of 54%, hence about half of the amplitude of the incident field is reflected. The next heavier construction is the clay block wall, which reflects about 83% of the field incident on it. The heaviest construction is the brick wall, but at 850 MHz, the average reflection coefficient is 69%, less than the clay block wall. The plaster-and-wire wall reflects 99.4% of the field, averaged over all angles for the “perpendicular” case. Note that the intuitive notion that heavier wall construction leads to a larger reflected field is incorrect and can be misleading. The fraction of the field that is reflected is dependent on the thickness of the various layers in the wall, on their electrical properties, on the angle of incidence, on the polarization, and on the frequency.

B. Ray Paths and Field Strengths

When only one receiver location is specified, GO_3D is used to study the ray paths coupling the transmitter and the receiver, and the associated field strength of each ray. With one receiver, GO_3D adds the ray paths to the plan and elevation view, as shown in Fig. 8. The electric field strength E_i associated with each ray is graphed as a function of the length of the ray path, as in Fig. 9. The path length axis is readily converted to time delay, by dividing by the speed of light, allowing the “delay spread” of rays arriving at the receiver to be assessed. An associated text file called “raylists.dat” is created by GO_3D. This file lists each ray found by the program, including all the reflection points associated with each ray, the field strength at the receiver, and the length of the ray path. The “raylists” file can be used to identify the paths of all of the rays shown in Figs. 8 and 9.

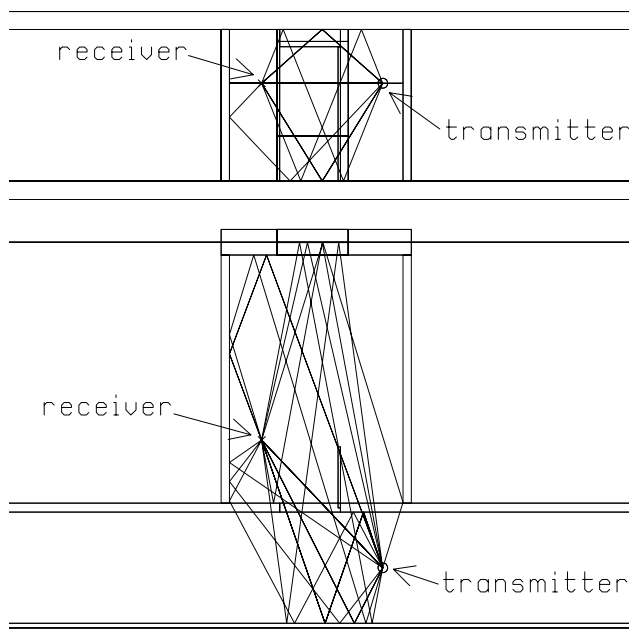


Fig. 8 A receiver with a line-of-sight path to the transmitter.

Fig. 8 shows a receiver positioned in the room near the left-hand wall, such that there is a line-of-sight path to the transmitter. A modest threshold of 10 dB has been used to draw the ray paths. If a more sensitive threshold is used, the program will draw so many rays that the usefulness of the ray path drawing is lost. Rays that are not transmitted through any wall often carry the largest field strengths. Fig. 8 clearly shows a “direct” ray that travels from the transmitter, through the doorway, to the receiver. There are four more rays passing through the open doorway. A ray travels from the transmitter, through the doorway, and then bounces from the room wall to arrive at the receiver. Another ray from the transmitter reflects from the hallway

wall opposite the door, and then travels through the doorway to the receiver. And there is a ray path that zig-zags, reflecting from the hallway wall near the door, then again from the hallway wall opposite the door, and then travels through the doorway to the receiver. The fourth ray travels from the source, reflects from the floor, and arrives at the receiver. Other rays are transmitted through the wall between the hallway and the room. There is a one-reflection path from the transmitter to the ceiling thence to the receiver but this ray passes through the transom above the door and so is attenuated by the transmission coefficient. Fig. 8 shows many ray paths that pass through the wall between the hallway and the room. Some of these rays bounce one or more times from the hall walls before passing into the room via transmission through the room walls. Some of the rays bounce from the room walls once or twice before reaching the transmitter. Quite a few rays bounce from the window glass, but this thin surface has a low reflection coefficient.

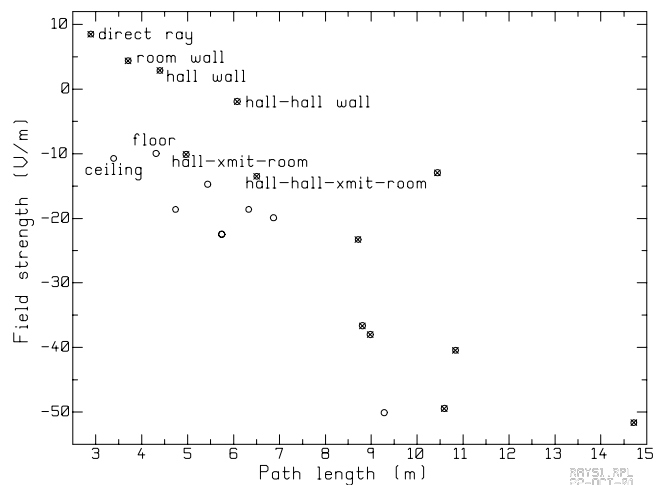


Fig. 9 The field strengths and path lengths for the rays at the line-of-sight observer.

Fig. 9 shows the field strength, in dB relative to 1 Volt/meter, associated with each of the rays arriving at the receiver, as a function of the ray path length. The circles show all the rays for a “three-dimensional” calculation, which includes the floor and the ceiling. To help in identifying ray paths, the same problem was run for a “two-dimensional” calculation by removing the floor and the ceiling from the problem, thus eliminating ray paths involving reflection from the floor or the ceiling. The “2D” ray paths are shown as crosses, so the circles without crosses are ray paths involving the ceiling or floor, or both. Because there is a line-of-sight path to the transmitter, the largest field strength is associated with the ray having the shortest path length of 2.9 m, called the “direct” ray. The next longer path length is the reflection from the ceiling. The directional pattern of the dipole transmitter reduces the field of rays directed upward. This ray also passes through

the wall above the doorway, with an associated transmission coefficient, and is attenuated by the ceiling reflection coefficient, so its field strength is 19 dB below the direct ray. The ray labeled “room wall” has the next longer path of 3.7 m has a single reflection from the room wall. The reflection from the floor has a path length of 4.3 m, but the field strength of this ray is small. The ray path labeled “hall wall” of path length of 4.4 m has a single reflection from the hall wall opposite the door and then passes through the doorway to the receiver. There is a ray labeled “hall-hall wall” in Fig. 9 that zigzags along the hall, with two reflections from the hall wall, then passes through the doorway to the receiver. A ray with a path length of about 5 m labeled “hall-xmit-room” reflects once from the hall wall, is transmitted through the room wall, and then reflects from the room side wall to reach the receiver. Due to the loss in transmission through the wall, the field strength associated with this ray is quite low. There is a ray labeled “hall-hall-xmit-room” which zig-zags along the hall, is transmitted through the hall wall into the room, and then reflects from the room wall to arrive at the receiver. Similarly, the “hall-xmit-room-room” ray reflects from the hall wall, is transmitted through the room wall into the room, then reflects twice from the room walls before reaching the receiver.

C. Field Strength with Increasing Threshold

The GO_3D program can compute the field strength along a straight-line path between any two points, such as the path from the center of the doorway to the window shown as a dashed line in Fig. 5. The program creates an output file giving E_x , E_y , E_z and E_t as a function of either distance along the line, or distance from the transmitter, as shown in Fig. 10.

The threshold field strength T (dB) is a control that lets the user determine how sensitive a calculation is carried out by the GO_3D program. As explained above, GO_3D does not ask the user to set a limit on the number of reflections that the program will track. Instead, the code retains all image sources that could, for some observer, give rise to fields that are larger than the “cutoff” field strength, which is T dB below the isotropic level field strength. GO_3D will track as many reflections as needed to meet this criterion.

For the hall with small room problem, with a 10 dB threshold, up to 7 reflections are tracked using a total of 426 image sources. With a 13 dB threshold, one more reflection is tracked and the number of image sources roughly doubles to 822. Note that the code does not find all the rays having 7 reflections, just those rays that might have field strength stronger than the threshold after 7 reflections. With a 16 dB threshold, up to 12 reflections are found using 1874 image sources. With a 19 dB threshold, 14 reflections are tracked using 7056 image sources. With a 22 dB threshold, 19 reflections are traced, using 26,037

image sources. With a 26 dB threshold the code tracks 29 reflections using 254,379 image sources.

Concerning execution time, the floor plan in Fig. 5 uses 14 wall panels including the floor and ceiling. A grid of about 9100 receivers was used as a test case. With a threshold of 10 dB, hence 426 sources, GO_3D uses about 30 seconds of CPU time. With a 16 dB threshold, hence 1874 sources, the program uses about three and a half minutes of CPU time. With a 22 dB threshold and 26,037 sources the program uses about three and a half hours of execution time. The program is not fully optimized for speed, and methods such as those in Ref. [5] or [6] could be used to speed the calculation.

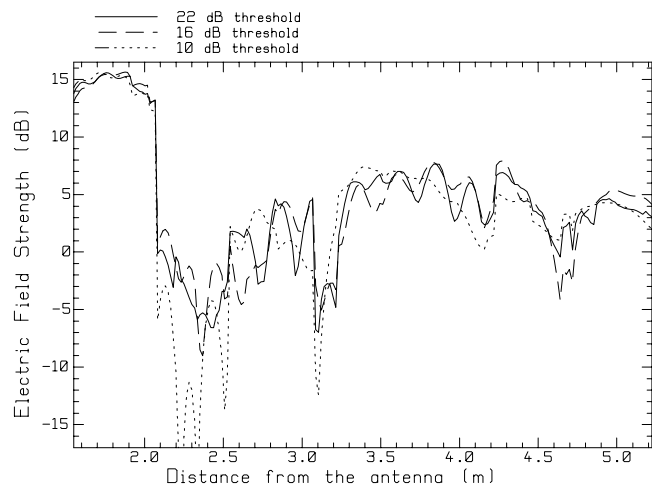


Fig. 10 The field strength along the path in Fig. 5, for various values of the threshold field strength.

Does the field become constant as the value of the threshold increases? Ideally, we would like the field to “converge” to a constant value as the threshold value is increased. But in general, this behavior is *not* found, as illustrated in Fig. 10. The figure shows the field strength E_z along the path in Figure 5 from the center of the door into the room to the window, using distance from the transmitter on the horizontal axis. The field is shown for thresholds of 10, 16, and 22 dB, values typical in the use of GO_3D. All three curves are similar overall; they are dominated by the few rays that have relatively large field strengths that are found by GO_3D even for the “low” 10 dB threshold value.

For close distances to the transmitter, there is a line-of-sight path from the transmitter to the observer and the behavior of the field is dominated by the large field strength of the “direct” ray from the transmitter, much like the case of Fig. 8 and 9. For all three threshold values, the field for distances less than 2.07 m is very similar. By increasing the threshold value, the user instructs the code to include additional rays with fields at a much lower level than the “direct” ray’s field, which have only a small effect on the net field strength.

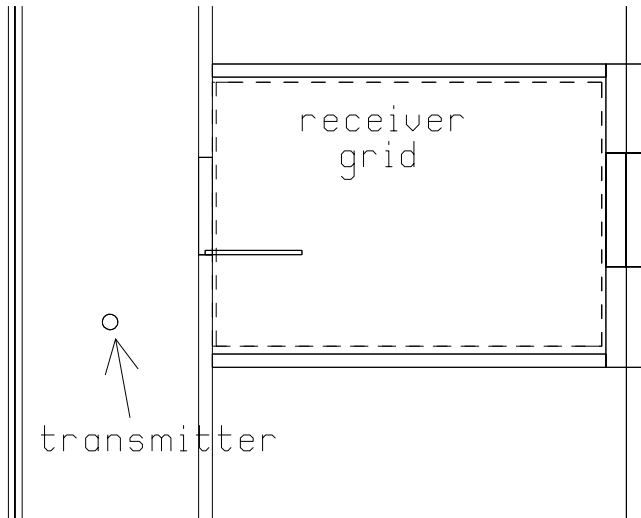


Fig. 11 The location of a grid of receivers in the room adjacent to the hallway.

At 2.07 m distance the line of sight path is blocked by the wall, and for larger distances the field is made up of rays reflected from the hall walls through the door, and rays that are transmitted through the hall wall, and then reflected from various room walls. With a 10 dB threshold only a modest number of rays contribute to the field, and there is a trough in the field strength from 2.07 m to 2.21 m distance. As the threshold is increased, a lot of “minor” rays are added which tend to fill in the trough, hence the field in this region with a 16 dB threshold is larger than with a 10 dB threshold. When even more “minor” rays are included by increasing the threshold to 22 dB, the field in this region is smoother but the average value is about the same as at 16 dB threshold.

From about 2.6 to 3.1 m distance, and again from about 3.5 to about 4.2 m, the field with a “low” 10 dB threshold is fairly smooth. Increasing the threshold to 16 dB adds the ripple to the field which is called “fast” fading. The average value of the field, the “slow fading”, is not much changed. Increasing the threshold to 22 dB affects the amplitude of the ripple, but again the “slow fading” or average value is not much changed.

The results shown in this figure are typical of those obtained by increasing the threshold value in GO_3D. The field does not “converge” to a value independent of the threshold at all. Instead, adding more image sources by increasing the threshold fills in troughs found with low threshold values, and adds “fast fading” behavior to the overall curve.

D. Fields On a Planar Grid

The GO_3D program can compute the field over an evenly-spaced grid of points parallel either to the xy , the xz or the yz plane. The program reports the value of the E_x ,

E_y , E_z and E_t field strengths in a tabular format as a function of the position on the grid. For example, suppose a 600 mW transmitter is operated in the hallway at the location shown in Fig. 11, which has been rotated by 90 degrees relative to Fig. 5. Suppose that equipment with an immunity of 3 V/m is to be operated somewhere in the room, which is covered with rectangular “receiver grid” shown in Fig. 11. GO_3D is to be used to assess whether the field in the room exceeds the immunity level.

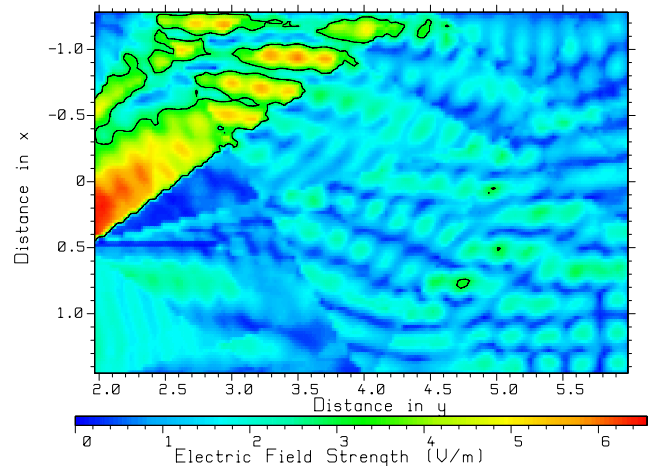


Fig. 12 The E_t component of the electric field strength in the room.

GO_3D was run to compute the field strength E_t over the grid of Fig. 11, with a threshold of 18 dB and a point spacing of 3.5 cm or about a tenth of a wavelength at 850 MHz. Fig. 12 shows a “color contour map” of the “total field” E_t . The point at $x=0$, $y=2$ m near the center at the left side of the map is at the center of the doorway into the room, and the field at this location is strong because it is “line of sight” to the transmitter. A beam of field flows into the room from the transmitter, upward and to the right, and reflects from the wall at the top of the figure, then flows downward and to the right into the room. There is a standing-wave pattern in the beam near the wall in the top quarter of the contour map, caused by interference of the ray reflected from the wall with the ray directly from the transmitter. Deeper in the room there is no line-of-sight path to the transmitter and the field is smaller in value, with colors from green through cyan to blue. The room contains an interference pattern showing maxima and minima that are oriented roughly horizontally on the page, and arise due to rays bouncing back and forth between the two walls of the room. The field behind the door, at the bottom left corner, is fairly uniform in value and arises mainly from a ray from the transmitter in the corridor that passes through the room wall into the room. The GO_3D program reports zero value for the field inside wall panels, such as inside the room door.

The 3 V/m field strength contour has been superimposed on the color map as a black contour line. The green, yellow and red regions within the contour have field strengths in excess of the immunity level of 3 V/m and so are unsafe for the operation of equipment, at least for the location of the transmitter in Fig. 11.

To determine locations in the hallway that lead to a maximum field strength over the receiver grid of less than 3 V/m, GO_3D provides a “transmitter grid” function. A grid of transmitter locations is defined in the hallway. At each transmitter location, the field over the whole receiver grid is calculated and the maximum value is found and recorded. Locations in the hall where this maximum field strength is less than the immunity are safe. This feature has been used to designate safe locations for cell phone operation in a hospital environment in Ref. [11].

V. Conclusions

This paper describes a ray-tracing program called GO_3D for indoor propagation problems. The user prepares an input file giving the floor plan and the materials and construction of the walls, the frequency and transmitter location, and the location of observers or “receivers”. The input “language” is intended to lead to a self-documenting file that is easy to read and modify. The user is encouraged to include comment lines in the file describing the contents, so that numbers in the file are readily traced to their source.

GO_3D computes the field strength either along a straight-line path defined by the user, or over a grid of points. The structure of the field in a region can be studied by drawing color contour maps of the field strength, as in Fig. 12. Using an observer at a single point, the GO_3D program creates output file that permit the study of the ray paths joining the transmitter to the receiver. Both the geometry of each ray, the length of the ray path and the field associated with it can be studied. Moving the observer in small steps permits the user to see which ray paths appear and disappear, and can be used to investigate and explain features found in contour maps of the field over a region.

GO_3D provides a control called the “threshold” which allows the user to determine the number of rays to be included in the calculation. The value of threshold required for a given problem depends on the wall construction and on whether energy can escape from the problem region. Thus, if a closed room were built with perfectly-reflecting walls, then rays will continue to bounce around inside the room indefinitely with no decrease in field strength, and the ray tracing method breaks down. If the room has walls that permit some energy to escape through them, then the field amplitude associated with each ray gradually decreases with each reflection, but rays may have to be traced through many reflections to obtain an accurate answer. Such a room is very “live”. Conversely, a “dead” room is one that

has many doorways and windows that allow rays to escape. Or a “dead” room might have walls that permit energy to penetrate through them, or that absorb energy, and in either case have a small reflection coefficient. In such a “dead” room, only a few reflections need to be traced.

There are various sources of error in the GO_3D calculation. GO_3D uses geometrical optics and so ignores diffracted rays from edges such as the corners of walls and doorways. Consequently, the field has discontinuities as rays “switch” on and off with changing observer position. Walls in GO_3D and other ray-tracing codes are modeled as uniform, layered structures. Internal details such as voids in clay blocks walls, studs of wood or metal, ducts, pipes and wiring are omitted. Large internal features such as a metal duct with flat surfaces might be explicitly included in the model as a metal wall panel. Small features such as pipes or wiring much smaller in diameter than the wavelength do not scatter specularly and so cannot be modeled with GO. Such features primarily affect the field in their immediate vicinity. The clutter of conduits, plumbing, wiring and ducts found above a typical hanging ceiling is another source of error. Large conduits scatter specularly and might be included in the model explicitly. The code could be extended to permit large circular pipes to be modeled explicitly. Smaller features, such as the metal angle used to support the hanging ceiling tiles, scatter the field rather than reflect it specularly. When the clutter above the ceiling tiles is neglected, then the ceiling reflects specularly, and this is clearly unrealistic. The error incurred is difficult to quantify. But the ceiling may not be omitted in a ray-tracing calculation, because this amounts to modeling the ceiling as a perfect absorber of energy. Perhaps some panels could be added between the height of the hanging ceiling and the height of the underside of the concrete slab of the floor above to approximate ducts and some other clutter, and break up the specular path from a smooth flat ceiling.

Room furnishings and people both scatter and absorb energy. Panels of lossy material could approximate furniture such as desks and chairs. Metallic panels could approximate scattering from file cabinets, for example. Lossy panels could approximate absorption by people. The authors are not aware of guidelines in the literature for choosing the size or electrical parameters appropriately, however. The speed of the calculation is strongly dependent on the number of panels that must be accounted for, so many small panels to model furniture and people would certainly slow down the calculation.

The accuracy of ray-tracing methods for indoor propagation is assessed in Ref. [7] relative to measured field strengths at 1.8 and 2.5 GHz. The authors conclude that ray-tracing calculations were able to estimate the Rician distribution of the received signal with good correspondence to the measured data. Ref. [7] includes first-order diffraction and diffraction-reflection, which make an important contribution when there is no line-of-

sight path. These terms are not included in the GO_3D code. Ref. [7] does not model furniture nor clutter above the hanging ceiling.

The GO_3D program could be used as a teaching tool in undergraduate or graduate courses dealing with wireless technology, antennas and indoor propagation. Students can gain some first-hand experience by modeling a specific indoor environment, to become aware of the major considerations. The input for the program is quite simple to prepare, starting from the sample problem in the User's Guide, and the program executes reasonably quickly on an inexpensive Pentium computer.

GO_3D has proven a useful tool for investigating the field in a room due to a transmitter located somewhere in the room, with reasonable correspondence to measurements [12]. The program has been used to study the decline in field strength with distance from the observer in long corridors [9]. The program has been used to study the locations in a corridor where a cellular telephone can be operated without exceeding the immunity level of equipment in an adjacent room [11], as in the example presented in this paper.

VI. Acknowledgements

The author acknowledges the contribution of Dr. Junsheng Zhao in implementing the layered-wall reflection and transmission coefficients of Ref. [10], as described in Ref. [13]. The author acknowledges his colleagues Dr. B. Segal and D. Davis for inspiration in developing the GO_3D code for the study of EMC problems in a hospital environment.

VII. References

1. International Electrotechnical Commission on Medical Equipment, *Part I: General Requirements for Safety, 2. Collateral Standard: Electromagnetic Compatibility*, 2nd edition, IEC 601-1-2, 1999.
2. C.A. Balanis, *Advanced Engineering Electromagnetics*, Wiley, New York, 1989.
3. M. Kimpe, H. Leib, O. Maquelin, and T. D. Szymanski, "Fast Computational Techniques for Indoor Radio Channel Estimation", *Computing in Science & Engineering*, pp. 31-41, Jan.-Feb., 1999.
4. C. Yang, B. Wu and C. Ko, "A Ray-Tracing Method for Modeling Indoor Wave Propagation and Penetration", *IEEE Trans. Antennas and Propagation*, Vol. AP-46, No. 6, pp. 907-919, June 1998.
5. O. Gutierrez, F. Saez de Adana, I. Gonzalez, J. Perez, M.F. Catedra, "Ray-Tracing Techniques for Mobile Communications", *Applied Computational Electromagnetics Society Journal*, Vol. 15, No. 3, pp. 209-231, November 2000.
6. Z. Ji, B-H Li, H-X Wang, H-Y Chen and T.K. Sarkar, "Efficient Ray-Tracing Methods for Propagation

Prediction for Indoor Wireless Communications", *IEEE Antennas and Propagation Magazine*, Vol. 43, No. 2, pp. 41-49, April 2001.

7. S. Lored, L. Valle, and R.P. Torres, "Accuracy Analysis of GO/UTD Radio-Channel Modeling in Indoor Scenarios at 1.8 and 2.5 GHz", *IEEE Antennas and Propagation Magazine*, Vol. 43, No. 5, pp. 37-50, October 2001.
8. E.H. Newman, *Plane Multilayer Reflection Code*, Technical Report 712978-1, ElectroScience Laboratory, The Ohio State University, July, 1980.
9. C.W. Trueman, *User's Guide for Program GO_3D*, Version 1J, Concordia University EMC Laboratory, October 18, 2001, http://www.ece.concordia.ca/~trueman/GO_3D/GO_3D_Users_Guide2.htm.
10. C.W. Trueman, D. Davis, and B. Segal, "Ray Optical Simulation of Indoor Corridor Propagation at 850 and 1900 MHz," *IEEE AP-S Conference on Antennas and Propagation for Wireless Communication*, pp. 81-84, Waltham, Massachusetts, November 6-8, 2000.
11. C.W. Trueman, D. Davis, and B. Segal, "Specifying Zones for Cellular Telephone Operation in Hospital Hallways," *Symposium on Antenna Technology and Applied Electromagnetics (ANTEM)*, pp. 381-386, Winnipeg, Manitoba, July 30-August 2, 2000.
12. C.W. Trueman, R. Paknys, J. Zhao, D. Davis, and B. Segal, "Ray Tracing Algorithm for Indoor Propagation," *ACES 16th Annual Review of Progress in Applied Computational Electromagnetics*, pp. 493-500, Monterey, California, March 20-24, 2000.
13. J. Zhao, R. Paknys, and C.W. Trueman, *Efficient Reflection and Transmission Dyad Multiplication for 3D Geometrical Optics*, Internal Report, EMC Lab, Concordia University, April, 2002.



Christopher W. Trueman

became a Lecturer at Concordia University, Montreal, Canada, in 1974 and received the Ph.D. degree from McGill University in 1979 with a thesis on wire-grid modeling aircraft and their HF antennas. His research in Computational Electromagnetics uses moment methods, the finite difference time domain method, and geometrical optics and diffraction. He has worked on EMC problems with standard broadcast antennas and high-voltage power lines, on the radiation patterns of aircraft and ship antennas, on EMC problems among the many antennas carried by aircraft, and on the calculation of the RCS of aircraft and ships. He has studied the near and far fields of cellular telephones operating near the head and hand. Recently he has been concerned indoor propagation of R.F. signals and EMI with medical equipment in hospital environments.